IL NUOVO CIMENTO Vol. 36 C, N. 6 Novembre-Dicembre 2013
DOI 10.1393/ncc/i2014-11649-x

Colloquia: LaThuile13

Measurements of the top-quark properties with the ATLAS detector

J. Yu on behalf of the ATLAS Collaboration

Oklahoma State University - Stillwater, OK, USA

ricevuto il 20 Giugno 2013; approvato l'1 Luglio 2013

Summary. — The top-quark discovered in 1995 is the third-generation up-type quark of the standard model (SM) of particle physics. Precise measurements of the top-quark properties at the Large Hadron Collider (LHC) energies are of great interest, providing an opportunity to test the SM and to search for new physics in the top-quark sector. This review covers the recent results from the ATLAS experiment on measurements of top-quark mass, top-quark polarization, spin correlation between top-quark and antitop-quark, $t\bar{t}\gamma$ cross section, W boson polarization in top-quark decays and searches for new physics in events with top-quarks in the final state. Measurements have been performed on data collected by the ATLAS detector corresponding up to $5\,\mathrm{fb}^{-1}$ of integrated luminosity at centre-of-mass energy of $\sqrt{s} = 7\,\mathrm{TeV}$.

PACS 14.65.Ha – Top quarks.

1. – Introduction

In proton-proton collisions at the LHC [1], top-quarks are mainly produced in pairs via strong interactions. Single top-quarks are produced via electroweak interactions. The top-quark is the most massive elementary particle ever found and has the strongest Yukawa coupling to the Higgs boson within the SM, implying a possible special role of the top-quark in the electroweak symmetry breaking mechanism. It has a very short lifetime and decays, before hadronizing, to a W boson and a b-quark with a probability close to 100%.

Experimentally, events with top-quarks fall into three categories according to the decay modes of the W boson: the leptop + jets channel, when one of the W bosons decays hadronically and another leptonically, the dilepton channel, when both W bosons decay leptonically, and the fully hadronic channel, when both W bosons decay to a pair of quarks. The lepton + jets final state provides a good balance between signal statistics and background contamination. The dilepton final state offers a cleaner signal sample with a lower statistic. The fully hadronic final state has the largest branching ratio but suffer from the highest background contamination.

This review presents results of the ATLAS [2] Collaboration on precision measurements of the top-quark properties at LHC energy of $\sqrt{s} = 7$ TeV in proton-proton collisions. Datasets corresponding up to 5 fb^{-1} were used, varying between measurements.

2. – Top-quark mass measurements

Top-quark mass (m_{top}) measurement in lepton + jets channel is performed using $1.04\,\text{fb}^{-1}$ of data applying the template fit method [3]. In a 2-dimensional fit method, m_{top} and a global jet energy scale factor (JSF) are determined simultaneously by using the reconstructed top mass (m_{top}^{reco}) and W boson mass (m_W^{reco}) distributions. This algorithm determines which global JSF correction should be applied to all jets to provide the best fit to data. Due to this procedure, the JSF is sensitive not only to the jet energy scale (JES), but also to all possible differences in data and predictions from specific assumptions made in the simulation that can lead to differences in observed and simulated jets. The top-quark mass measured with this method is $m_{top} = 174.5 \pm 0.6$ (stat.) $\pm\, 2.3$ (syst.) GeV. The main sources of systematic uncertainties are the residual JES uncertainty and the uncertainty on the b-jet energy scale, and the modelling of initial and final state radiation.

Measurement of the top-quark mass in dilepton channel is performed on data corresponding to $4.7\,\text{fb}^{-1}$ of integrated luminosity [4]. Experimentally, the distribution of the variable m_{T2} defined as in the following eq. (1) was examined. The m_{T2} variable is used in cases in which each parent particle decays into visible particles and one undetected (invisible) particle:

$$M_{T2} \equiv \min_{\vec{p_T}^{\nu_1}, \vec{p_T}^{\nu_2}} \{\text{Max}[M_T(m_{lb_1}, \vec{p_T}^{\nu_1}), M_T(m_{lb_2}, \vec{p_T}^{\nu_2})]\}, \tag{1a}$$

where

$$M_T(m_{lb_i}, \vec{p_T}^{\nu_j}) \equiv \sqrt{m_{lb_i}^2 + m_{\nu_j} + 2(E_T^{lb_i} E_T^{\nu_j} - p_T^{\vec{lb}_i} p_T^{\vec{\nu}_j})}. \tag{1b}$$

The mean value of the m_{T2} distribution, $\overline{m}_{T2}$, observed in data with background subtracted depends on the top-quark mass, where the dependence is described by the calibration curve (fig. 1, left). It is obtained using MC simulation samples to map the observable, $\overline{m}_{T2}$, into m_{top}. The m_{T2} distribution is shown in fig. 1 (right). The measured top mass is found to be $m_{top} = 175.2 \pm 1.6$ (stat.)$^{+3.1}_{-2.8}$ (syst.) GeV.

The top-quark mass is also measured in fully hadronic decays [5]. Result is found to be $m_{top} = 174.9 \pm 2.1$ (stat.) $\pm\, 3.8$ (syst.) GeV, compatible with the one obtained in the dilepton channel.

3. – Measurement of the top-quark polarization

In the SM, top-quarks are produced unpolarized, while some models beyond the SM (BSM) predict a measurable polarization of the top-quark. In particular, models that predict the top-quark forward-backward asymmetry to be larger than the SM prediction, as observed at Tevatron [6], have different predictions of the top-quark polarization [7].

A distribution of $\cos\theta_l$ is obtained by fully reconstructing $t\bar{t}$ system in the lepton + jets final state, where θ_l is the polar angle of the lepton in the top-quark rest frame. Templates are created from MC signal events, correpsonding to fully positive polarization

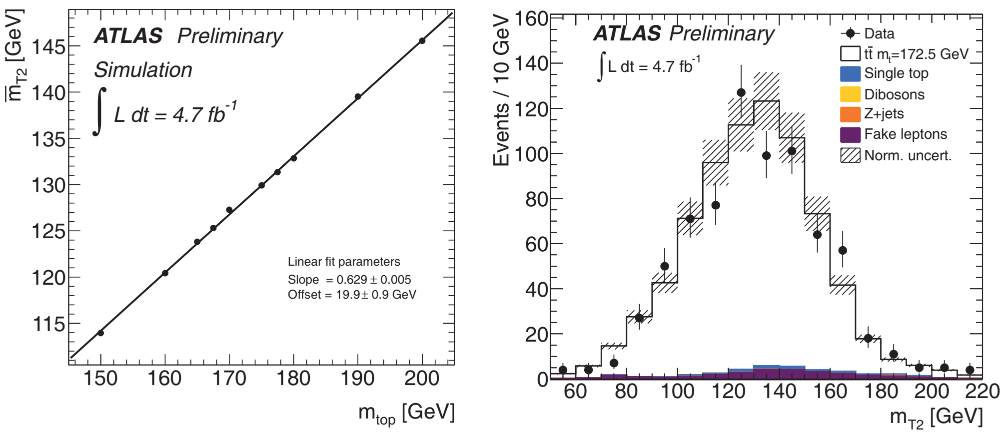

Fig. 1. – The calibration curve (left) determined in MC showing the dependence of the m_{T2} on m_{top} and the distribution of the m_{T2} in MC and data (right) in the dilepton $e\mu$ channel [4].

$(1 + \cos\theta_l)$ and fully negative polarization $(1 - \cos\theta_l)$, including the templates from background events. A fit of the reconstructed $\cos\theta_l$ distribution is thereafter performed to extract the fraction of positively polarized top-quarks, f.

The distribution of $\cos\theta_l$ and the data fitting templates are shown in fig. 2 for μ + jets channel.

The results of the fit is found to be $f = 0.470 \pm 0.009$ (stat.)$^{+0.023}_{-0.032}$ (syst.) [8], in the combined lepton + jets channel. It is compatible with the SM prediction of unpolarized model $f_{SM} = 0.5$.

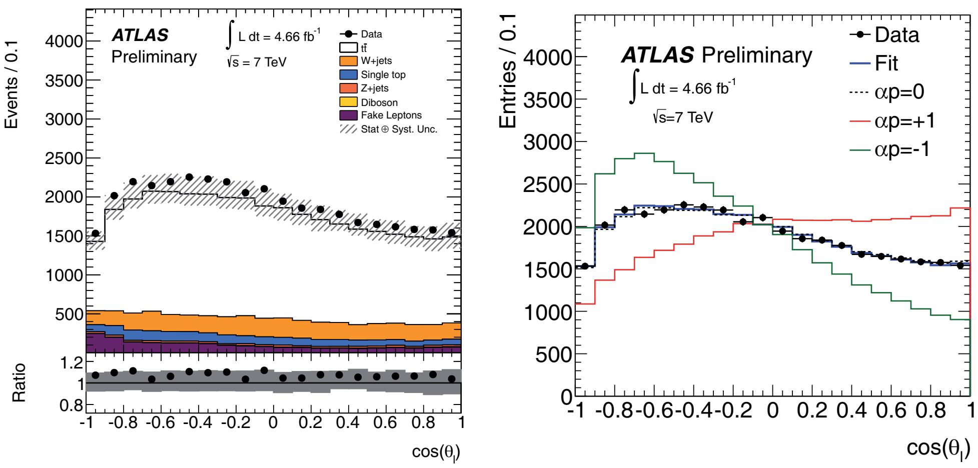

Fig. 2. – The distribution of $\cos\theta_l$ in data is overlayed with the prediction in MC, where top-quarks in $t\bar{t}$ production are not polarized (left). A fit is performed using positive and negative polarization top-quark templates (right). Both are for μ + jets channel. Corresponding plots for e + jets channel can also be found in the paper of the top-quark polarization [8].

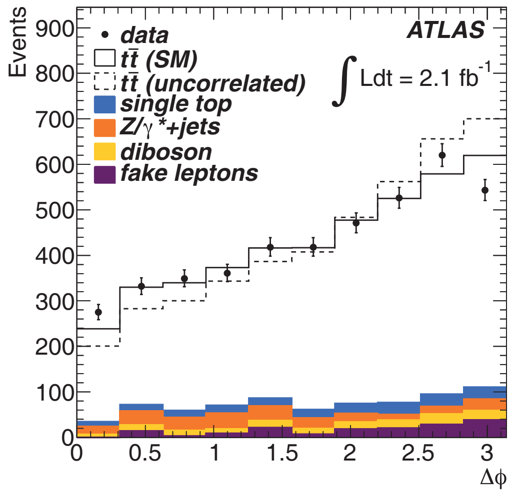

Fig. 3. – Reconstructed $\Delta\phi$ distribution in data compared with the SM prediction and a model with uncorrelated spins [9]. The integrated number of events for both the SM and the uncorrelated ttbar samples is fixed to the value from the fit. MC background samples are either normalized to their predicted cross sections or from data driven measurements.

4. – Measurement of the spin correlation in top-quark pair production

Due to the short lifetime of the top-quark that does not allow it to hadronize, the information of its spin is transferred to the decay products. Measurement of the top and antitop spin correlation had been performed in the dilepton channel using the informantion on the distribution of azimuthal angle of two leptons ($\Delta\phi$) [9] and compared to the SM expected value.

The degree of correlation is defined in the following eq. (2), as the fractional difference between the number of events with the top-quark and antitop-quark spin orientations aligned in the same direction and those aligned oppositely:

$$A \equiv \frac{N(\uparrow\uparrow) + N(\downarrow\downarrow) - N(\uparrow\downarrow) - N(\downarrow\uparrow)}{N(\uparrow\uparrow) + N(\downarrow\downarrow) + N(\uparrow\downarrow) + N(\downarrow\uparrow)}. \tag{2}$$

The templates are constructed using simulated $t\bar{t}$ events and combined to a linear superposition of the one from SM with coefficient f_{SM} and the other from the uncorrelated model with coefficient $(1 - f_{SM})$. A template fit to the $\Delta\phi$ distribution in data is used to determine the amount of spin correlation. The distribution of the reconstructed $\Delta\phi$ is shown in fig. 3.

The fit results in $f^{SM} = 1.30 \pm 0.14$ (stat.)$^{+0.27}_{-0.22}$ (syst.), which is converted into a value of A in two bases: the helicity basis [10], $A^{measured}_{helicity} = 0.40 \pm 0.04$ (stat.)$^{+0.08}_{-0.07}$ (syst.), and the maximal basis [11], $A^{measured}_{maximal} = 0.57 \pm 0.06$ (stat.)$^{+0.12}_{-0.10}$ (syst.). The results are compatible with the theoretical prediction $A^{SM}_{helicity} = 0.31$ [12] and $A^{SM}_{maximal} = 0.44$, and are inconsistent with the hypothesis of zero spin correlation with a significance of 5.1 standard deviations.

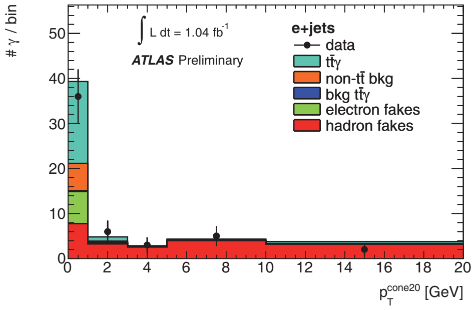

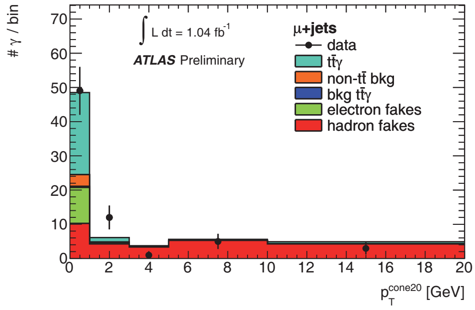

Fig. 4. – The distribution of p_{T}^{cone20} of the photon in the $t\bar{t}\gamma$ cross section measurement [13]. These distributions are after the template fit in e + jets channel (left) and μ + jets channel (right). The predicted $t\bar{t}\gamma$ signal is shown on top of the different background contributions.

5. – Measurement of the $t\bar{t}\gamma$ production cross section

The electroweak couplings of the top quark can be probed directly by investigating $t\bar{t}$ events with an additional gauge boson, like $t\bar{t}\gamma$ and $t\bar{t}Z$. A search for $t\bar{t}Z$ candidates in the three lepton final state with $4.7\,\mathrm{fb}^{-1}$ of data in ATLAS was presented in [14]. The result of the search sets a 95% upper limit of 0.71 pb on the $t\bar{t}Z$ production cross section, consistent with the next-to-leading-order (NLO) SM prediction of 0.14 pb [15]. A discovery or exclusion of $t\bar{t}Z$ production requires a larger dataset collected by ATLAS at $\sqrt{s} = 8\,\mathrm{TeV}$ in 2012. This proceeding describes in more details the $t\bar{t}\gamma$ production cross section measurement [13].

In addition to the $t\bar{t}$ event topology, the $t\bar{t}\gamma$ event selection requires a well identified photon with a transverse energy of exceeding 15 GeV. In the e + jets channel, it is further required that the invariant mass of the electron and photon is outside of a ± 5 GeV mass window around the Z boson mass to reject $Z \to e^+e^-$ background.

The $t\bar{t}\gamma$ cross section measurement is done using template fit to the p_{T}^{cone20} distribution of photon candidates, where p_{T}^{cone20} is defined as the scalar sum of transverse momenta of all tracks in a cone of $R < 0.2$ centered around the photon direction. The photon candidates from the signal events are isolated. Therefore, p_{T}^{cone20} (shown in fig. 4) is expected to be close to 0.

In the e + jets and μ + jets samples, 52 and 70 candidate events have been identified in data for an integrated luminosity of $1.04\,\mathrm{fb}^{-1}$. With the template fit, the numbers of events of signal and total background are found to be 46 ± 12 and 78 ± 14 with their statistical uncertainties in the combined lepton + jets channel.

The fitted results of $t\bar{t}\gamma$ cross section in e + jets and μ + jets channels are consistent within the statistical uncertainty. The $t\bar{t}\gamma$ cross section times the branching ratio ($\mathcal{B}$) of $t\bar{t}$ dilepton and lepton + jets decay modes is measured to be $\sigma_{t\bar{t}\gamma} \times \mathcal{B} = 2.0 \pm 0.5$ (stat.) $\pm$ 0.7 (syst.) $\pm$ 0.08 (lumi.) pb. It is consistent with the SM prediction 2.1 ± 0.4 pb [16].

6. – Measurement of the W boson helicity fractions

The Wtb vertex Lorentz structure and couplings in SM can be probed by measuring the polarization of W bosons produced in top-quark decays. In the SM, the Wtb vertex has a $(V - A)$ structure, where V and A are the vector and axial-vector contributions

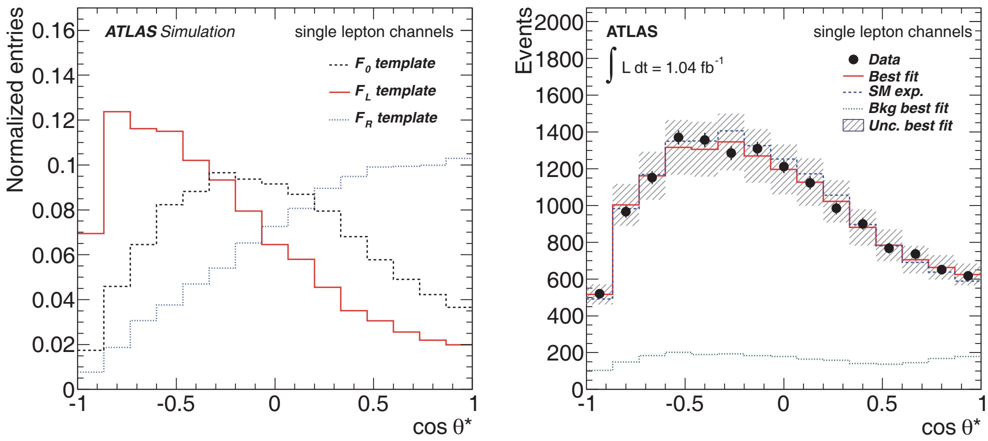

Fig. 5. – The distributions of reconstructed $\cos\theta^*$ for each of the three simulated signal templates (left) are used for W helicity measurement [18]. The distributions for data, the Standard Model prediction and the best fit value (right) are shown for lepton + jets channel.

to the vertex. The W bosons produced in top-quark decays may have longitudinal, left-handed or right-handed polarizations with corresponding probabilities F_0, F_L and F_R. Next-to-next-to-leading-order (NNLO) QCD calculations in SM result in following values of fractions $F_0 = 0.687 \pm 0.005$, $F_L = 0.311 \pm 0.005$, $F_R = 0.0017 \pm 0.0001$ [17].

W helicity fractions are measured using two different methods, the template fit method and the angular asymmetry method, with data corresponding to $1.04\,\text{fb}^{-1}$ of integrated luminosity [18]. Both measurements are done in lepton + jets and dilepton channels.

In the template fit method, the fractions, F_0, F_L and F_R, are extracted from fits to the $\cos\theta^*$ distribution in data, where θ^* is defined as an angle between the charged lepton momentum direction and the reversed b-quark momentum direction, both boosted into the W boson rest frame. $\cos\theta^*$ is related to the W helicity fractions through the following equation:

$$\frac{1}{\sigma}\frac{\mathrm{d}\sigma}{\mathrm{d}\cos(\theta^*)} = \frac{3}{4}(1-\cos^2\theta^*)F_0 + \frac{3}{8}(1-\cos\theta^*)^2 F_L + \frac{3}{8}(1+\cos\theta^*)^2 F_R. \tag{3}$$

Three signal templates are generated with MC assuming $F_0 = 1$, $F_L = 1$ and $F_R = 1$. Templates obtained on lepton + jets events are shown in fig. 5 (left). Results of the fit to the data with sum of templates are shown in fig. 5 (right).

In the method of the angular asymmetry, the $\cos\theta^*$ distribution is divided into four non-uniform bins, which were used to calculate the angular asymmetries ($A^{\pm}$), as defined in the following:

$$A_{\pm} = \frac{N(\cos\theta^* > z_{\pm}) - N(\cos\theta^* < z_{\pm})}{N(\cos\theta^* > z_{\pm}) + N(\cos\theta^* < z_{\pm})}, \quad \text{where} \quad z_{\pm} = \pm(1-2^{2/3}). \tag{4}$$

TABLE I. – *The W helicity fractions measured with methods of template fit and angular asymmetry* [18]. *These are compared to the predicted values in SM.*

W helicity fraction	Longitudinal (F_0)	Left-handed (F_L)	Right-handed (F_R)
SM prediction	0.687 ± 0.005	0.311 ± 0.005	0.0017 ± 0.0001
Template fit	$0.66 \pm 0.06 \pm 0.07$	$0.33 \pm 0.03 \pm 0.03$	$0.01 \pm 0.03 \pm 0.06$
Angular asymmetry	$0.67 \pm 0.04 \pm 0.07$	$0.32 \pm 0.04 \pm 0.02$	$0.01 \pm 0.02 \pm 0.04$

An iterative unfolding procedure is applied to data after background subtraction to extract the helicity fractions. The results for angular asymmetries are $A_+ = 0.52 \pm 0.02(\text{stat.}) \pm 0.03$ (syst.) and $A_- = -0.84 \pm 0.01$ (stat.) ± 0.02 (syst.) in the lepton + jets channel. Similar results are found in the dilepton channel with slightly larger statistical and systematic uncertainties.

The results of the W helicity fractions are presented in table I. for both methods in the combined lepton + jets and dilepton channels. The results are consistent with the SM prediction and are further combined using the best linear unbiased estimator ($BLUE$) method [19, 20]. The overall combination and the list of the results in the two methods in ATLAS are summarized in fig. 6.

7. – New physics search

Various BSM searches in the top-quark sector have been performed; no evidence of deviation from the SM has been found so far.

Searches for flavor changing neutral current (FCNC) processes have been performed in the top-quark production processes [21] as well as in top-quark decays [22]. Results are quoted in terms of upper limits on the branching ratio of the top-quark decay $\mathcal{B}(t \to ug) < 5.7 \times 10^{-5}$ and $\mathcal{B}(t \to cg) < 2.7 \times 10^{-4}$ and $\mathcal{B}(t \to Zq) < 7.3 \times 10^{-3}$.

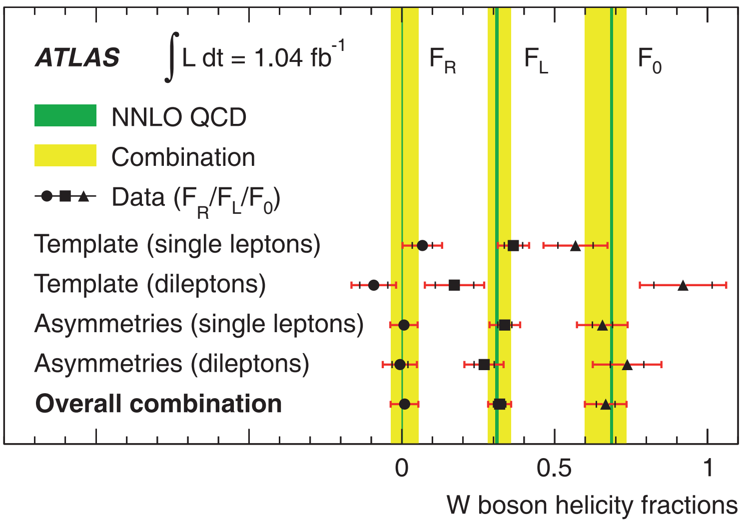

Fig. 6. – Input measurements and the combination of the W helicity results in ATLAS with $BLUE$ method [19, 20]. The error bars correspond to the statistical and total uncertainties [18].

Several new heavy quark production searches are also performed, including up-type and down-type fourth generation quarks [23,24], single or pair production of $T_{5/3}$ (heavy top-quark partner with electric charge $\pm 5/3$) [25], excited heavy b^* quark [26]. As an example, in the search for $b^* \to tW$, the most stringent lower limit so far at the LHC is set to $m_{b^*} > 870\,\text{GeV}$ with purely left-handed couplings and unit strength chromomagnetic coupling.

Additional results and updates are available from the ATLAS top group public results webpage [27].

8. – Conclusion

In this proceeding, a collection of recent measurements of top-quark properties from the ATLAS experiment, using up to $5\,\text{fb}^{-1}$ of data taken at $\sqrt{s} = 7\,\text{TeV}$, has been presented. Measurements are in agreement with the SM predicitons and no evidence of new physics has been found yet.

In 2012, ATLAS has collected more than $21\,\text{fb}^{-1}$ data at $\sqrt{s} = 8\,\text{TeV}$. With the better understanding of the detectors and the increasing centre-of-mass energy and the statistics, more precise results of the top-quark properties will be presented in the coming years, which will highly improve our understanding of the top-quark properties.

* * *

This proceeding is supported by the ATLAS Collaboration. I would like to thank the LHC personally for the smooth running of the machine and my colleagues from ATLAS experiment for the efficient data taking, calibration and analyzing of the data.

REFERENCES

[1] Evans L. and Bryant P. (Editors), *JINST*, **3** (2008) S08001.
[2] The ATLAS Collaboration, *JINST*, **3** (2008) S08003.
[3] The ATLAS Collaboration, *Eur. Phys. J. C*, **72** (2012) 2046.
[4] The ATLAS Collaboration, ATLAS-CONF-2012-082, `https://cdsweb.cern.ch/record/1460394`.
[5] The ATLAS Collaboration, ATLAS-CONF-2012-030, `https://cdsweb.cern.ch/record/1431895`.
[6] The DØ Collaboration, *Phys. Rev. D*, **84** (2011) 112005, arXiv:1107.4995[hep-ex].
[7] Krohn D., Liu T., Shelton J. and Wang L.-T., *Phys. Rev. D*, **84** (2011) 074034, arXiv:1105.3743[hep-ph].
[8] The ATLAS Collaboration, ATLAS-CONF-2012-133, `https://cdsweb.cern.ch/record/1478373`.
[9] The ATLAS Collaboration, *Phy. Rev. Lett.*, **108** (2012) 212001.
[10] Hubaut F., Monnier E., Pralavorio P., Smolek K. and Simak V., *Eur. Phys. J. C*, **44S2** (2005) 13.
[11] Uwer P., *Phys. Lett. B*, **609** (2005) 271.
[12] Bernreuther W. and Si Z. G., *Nucl. Phys. B*, **837** (2010) 90.
[13] The ATLAS Collaboration, ATLAS-CONF-2011-153, `https://cdsweb.cern.ch/record/1398197`.
[14] The ATLAS Collaboration, ATLAS-CONF-2012-126, `https://cdsweb.cern.ch/record/1474643`.
[15] Kardos A., Trócsányi Z. and Papadopoulos C., *Phys. Rev. D*, **85** (2012) 054015, arXiv:1111.0610[hep-ph].

[16] Melnikov K., Schulze M. and Scharf A., *Phys. Rev. D*, **83** (2011) 074013, arXiv:1102.1967[hep-ph].
[17] Czarnecki A., Korner J. G. and Piclum J. H., *Phys. Rev. D*, **81** (2010) 111503, arXiv:1005.2625[hep-ph].
[18] The ATLAS Collaboration, *JHEP*, **1206** (2012) 088.
[19] Lyons L., Gibaut D. and Clifford P., *Nucl. Instrum. Methods A*, **270** (1988) 110.
[20] Valassi A., *Nucl. Instrum. Methods A*, **500** (2003) 391.
[21] The ATLAS Collaboration, *Phys. Lett. B*, **712** (2012) 351-369.
[22] The ATLAS Collaboration, *JHEP*, **09** (2012) 139.
[23] The ATLAS Collaboration, *Phys. Lett. B*, **718** (2013) 1284-1302.
[24] The ATLAS Collaboration, *Phys. Rev. Lett.*, **109** (2012) 032001.
[25] The ATLAS Collaboration, ATLAS-CONF-2012-130, `https://cdsweb.cern.ch/record/1478217`.
[26] The ATLAS Collaboration, *Phys. Lett. B*, **721** (2013) 171.
[27] The ATLAS Collaboration, Top group public results webpage: `https://twiki.cern.ch/twiki/bin/view/AtlasPublic/TopPublicResults`.